PHYSICS OF PLASMAS 17, 055706 (2010)

Driven magnetic reconnection near the Dreicer limit[a)]

V. Roytershteyn,[1,b)] W. Daughton,[1] S. Dorfman,[2] Y. Ren,[2] H. Ji,[2] M. Yamada,[2] H. Karimabadi,[3] L. Yin,[1] B. J. Albright,[1] and K. J. Bowers[1,c)]
[1]*Los Alamos National Laboratory, Los Alamos, New Mexico 87545, USA*
[2]*Center for Magnetic Self-organization in Laboratory and Astrophysical Plasmas, Princeton Plasma Physics Laboratory, Princeton, New Jersey 08543, USA*
[3]*University of California, San Diego, La Jolla, California 92093, USA*

(Received 20 November 2009; accepted 30 March 2010; published online 6 May 2010)

The influence of Coulomb collisions on the dynamics of driven magnetic reconnection in geometry mimicking the Magnetic Reconnection eXperiment (MRX) [M. Yamada *et al.*, Phys. Plasmas **4**, 1936 (1997)] is investigated using two-dimensional (2D) fully kinetic simulations with a Monte Carlo treatment of the collision operator. For values of collisionality typical of MRX, the reconnection mechanism is shown to be a combination of collisionless effects, represented by off-diagonal terms in the electron stress tensor, and collisional momentum exchange between electrons and ions. The ratio of the reconnection electric field E_R to the critical runaway field $E_{\rm crit}$ provides a convenient measure of the relative importance of these two mechanisms. The structure of electron-scale reconnection layers in the presence of collisions is investigated in light of the previously reported [S. Dorfman *et al.*, Phys. Plasmas **15**, 102107 (2008)] discrepancy in the width of the electron reconnection layers between collisionless simulations and experimental observations. It is demonstrated that the width of the layer increases in the presence of collisions, but does not substantially deviate from its collisionless values, given by the electron crossing orbit width, unless $E_R \ll E_{\rm crit}$. Comparison with MRX observations demonstrates that the layer width in 2D simulations with Coulomb collisions is substantially smaller than the value observed in the low-density experiments with $E_R \lesssim E_{\rm crit}$, indicating that physical mechanisms beyond those included in the simulations control the structure of the electron layers in these experiments. © *2010 American Institute of Physics*. [doi:10.1063/1.3399787]

I. INTRODUCTION

Magnetic reconnection is an ubiquitous phenomenon involving a rapid change in the magnetic field topology, which is frequently accompanied by conversion of magnetic field energy into plasma kinetic energy. This process is thought to play a key role in the dynamics of many systems in nature under a wide range of plasma conditions. Important examples of such systems include Earth's magnetosphere, the solar atmosphere, and laboratory fusion experiments. Significant progress in understanding of magnetic reconnection has been made, but many important basic questions remain open. Progress on certain key issues has been hampered by difficulties in using observations and experimental measurements to discriminate between various theoretical models. For example, satellite observations provide a wealth of *in situ* information about collisionless reconnection in Earth's magnetosphere and the solar wind, but the measurements are necessarily limited to a few isolated spatial locations and unraveling the full structure and physics of reconnection layers remains challenging. Dedicated laboratory experiments offer the advantage of a controlled environment and repeatable local measurements but typically operate in regimes that are different from those in many systems of interest, as signified, for example, by the representative values of the Lundquist number and the ratio between the characteristic size of the system and kinetic scales (e.g., ion inertial length or ion gyroradius). Computer simulations potentially offer a bridge between the laboratory and other systems of interest, allowing the results of experimental observations to be extrapolated to different parameter regimes, and even helping guide the design of new experiments. However, a careful comparison between the simulation results and the experimental observations for the range of parameters typical of the experiments is crucial in order for these goals to be realized.

In this paper we report the latest results from an ongoing effort to perform direct comparison of fully kinetic simulations with experimental observations from the Magnetic Reconnection eXperiment (MRX).[1] MRX is a compact toroidal device where the reconnection is driven by reducing the current in two toroidal coils (in so-called *pull* scenario), which leads to the formation of a narrow reconnection layer between the coils. Recent improvements in the diagnostics have enabled detailed measurements of the structure of the electron-scale layers.[2–5] These measurements indicate that the half thickness δ of the electron layer in MRX is $(5.5-7.5)d_e$, where $d_e = c/\omega_{pe}$ is the electron skin depth and ω_{pe} is the plasma frequency. In contrast, recent two-dimensional (2D) collisionless simulations of MRX found $\delta = (2-3)d_e$.[6] Since the width of the layer is thought to be related to the reconnection mechanism, this discrepancy

[a)]Paper BI2 3, Bull. Am. Phys. Soc. **54**, 20 (2009).
[b)]Invited speaker.
[c)]Guest scientist. Present address: D. E. Shaw Research, LLC, New York, New York 10036.

likely indicates that the reconnection mechanism is different between the collisionless simulations and the experiment. The present work extends the analysis of Ref. 6 and investigates the influence of Coulomb collisions on the dynamics of magnetic reconnection for plasma parameters mimicking MRX. The MRX experiments span a rather wide range of collisionality regimes. In fully collisional regimes the reconnection electric field in MRX is supported by collisional momentum exchange between electrons and ions and the value of the effective resistivity η_{eff}, defined as the ratio between the reconnection electric field and the current density, is close to the Spitzer value.[7] In weakly collisional regimes the characteristic width of the reconnection layer is below the ion kinetic scales (ion inertial length and ion gyroradius) and the effective resistivity significantly exceeds the Spitzer value.[8–11] The exact nature of the effective resistivity enhancement in experiments is not understood, with two leading candidates being onset of two-fluid effects and possibly of anomalous dissipation induced by electromagnetic fluctuations.

Uncovering the origin of the observed value of η_{eff} is one of the ultimate objectives of the effort to perform detailed comparisons between simulations and the experiments since this may provide important insights into the mechanisms producing magnetic reconnection in other environments of interest. The focus of the analysis presented in this paper is to understand if 2D kinetic simulations with Coulomb collisions and realistic boundary conditions can account for the observed layer structure in MRX. The employed simulation technique utilizes a fully kinetic description for all plasma species and a Monte Carlo model for the collision operator. This enables a rigorous treatment of regimes with arbitrary collisionality, including the crossover between the collisionless and collisional regimes. In the latter case the use of fluid models may become problematic since the reconnection electric field may approach or exceed the runaway limit, while the magnitude of the reconnection flows and the characteristic length scales for the variations of magnetic field, density, and temperature push against the limits of validity of the classical transport theory.[12] In addition, accurate treatment of the Coulomb collisions correctly captures all the physics of the collisional momentum exchange (e.g., the thermal force), which may be important for reconnection,[13] but is typically not included in the fluid models.

The subject of magnetic reconnection in weakly collisional regimes has received considerable attention over the years (e.g., Refs. 14–17). These studies have been mostly focused on identifying parametric transitions between MHD and two-fluid regimes in relatively simple 2D configurations. In both of these regimes, the reconnection electric field is relatively small and is supported by resistivity or electron viscosity. On the other hand, a combination of MRX and kinetic simulations offers a unique opportunity to systematically study the physics of reconnection in the *runaway regime*, where the electric field is of the order of the Dreicer[18] limit. This virtually unexplored regime is of direct relevance to reconnection in the sun's atmosphere, where there are many outstanding questions regarding the basic properties of reconnection process, the effectiveness of bulk heating versus energetic particle generation, and the generation and role of various kinetic instabilities. In this paper, we concentrate on the problem immediately relevant to resolving the discrepancy between collisionless simulations and MRX observations, namely, on the width of the electron layers and its relation to the reconnection mechanism. Since a detailed comparison of the collisionless simulations with experimental observations was reported in Refs. 3–6, we focus on quantifying the changes in the width of the layer with collisionality.

The organization of this paper is as follows. The computational model is introduced in Sec. II. Section III is dedicated to the discussion of the dependence of reconnection rate on the strength of the drive and the value of collisionality. The simulations demonstrate that in a manner qualitatively similar to the experiment[8–10,19] the reconnection mechanism, as represented by the dominant terms in the generalized Ohm's law, varies continuously from fully collisional regimes, where the momentum exchange between electrons and ions dominates, to collisionless regimes where the relevant effects are represented by off-diagonal terms in the electron stress tensor. A natural way of identifying the reconnection regime is offered by the ratio of the reconnection electric field to the critical runaway field. In Sec. IV, the influence of Coulomb collisions on the structure of the electron layer is examined. It is demonstrated that collisions do not broaden the width of the layer measured in terms of an appropriately defined gyroradius unless the reconnection field is substantially smaller than the runaway limit. This implies that the width of the layer predicted by simulations is significantly below values observed in low-density MRX discharges. The results are summarized and implications are discussed in Sec. V.

II. COMPUTATIONAL MODEL

The 2D simulations described in this paper were carried out using the high-performance particle-in-cell (PIC) code VPIC.[20,21] This fully kinetic explicit PIC code solves the Maxwell equations coupled to the Boltzmann equation for each plasma species, which in the nonrelativistic limit of interest may be written as

$$\partial_t f_s + \boldsymbol{v}\cdot\nabla f_s + \frac{q_s}{m_s}\left(\boldsymbol{E}+\frac{1}{c}\boldsymbol{v}\times\boldsymbol{B}\right)\cdot\nabla_v f_s = \sum_{s'}\mathbb{C}\{f_s,f_{s'}\}. \tag{1}$$

Here $\mathbb{C}\{f_s,f_{s'}\}$ is the collision operator between species s and s' and the other symbols have their usual meaning. The Coulomb collisions are modeled using the Takizuka–Abe particle-pairing algorithm,[22] which in the limit of large number of particles per computational cell and small time steps reproduces the full Landau collision integral. The VPIC implementation of the collision algorithm has been extensively benchmarked[13,23] and recently applied to studies of magnetic reconnection in neutral sheet geometry.[13,24] Although computationally expensive, this technique allows the

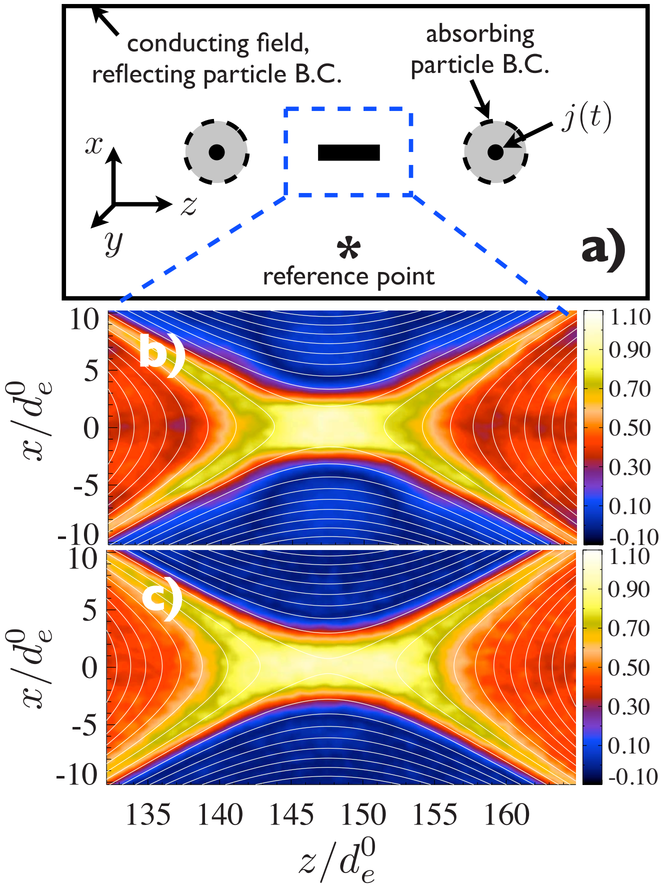

FIG. 1. (Color online) (a) The geometry of the simulation domain. Boundary conditions are conducting for the fields and reflecting for the particles at the outer walls. Two current-carrying regions of the simulation, denoted by black disks, create the in-plane magnetic field. They are housed inside flux cores, which are denoted by gray disks and are absorbing for the particles. The asterisk marks the reference point where B_0 is prescribed. (b) Current density j_y in a collisionless simulation with $m_i/m_e=100$, $n_0=2\times 10^{13}$ cm^{-3}, and $\tau\Omega_{ci}^0=300$. (c) Current density j_y in a simulation with the same parameters, but with $\nu_e/\Omega_{ce}\approx 0.03$. In both cases j_y is normalized to its peak value. The white lines show isocontours of the magnetic flux.

reconnection in weakly coupled regimes with arbitrary collisionality to be analyzed.

The simulation geometry and boundary conditions closely resemble those described in Ref. 6. As illustrated in Fig. 1, the simulation domain consists of a rectangular box of size (150×75) cm, with conducting boundary conditions for electromagnetic field and reflecting boundary conditions for particles at the walls. The MRX flux cores housing poloidal and toroidal coils are modeled entirely through particle boundary conditions, chosen to be fully absorbing. This choice of the boundary conditions is discussed in detail and motivated in Ref. 6. The particle boundary conditions at the flux cores are potentially important since they may affect the buildup of pressure in the downstream region, which is known to be an important parameter in MRX.[25] In the real device the region near the flux core is dominated by the processes of plasma formation and notoriously complicated plasma-wall interactions. Instead of being a detailed model of these processes, the flux core particle boundary conditions in the simulations should be viewed as a way of manipulating the downstream pressure. The results presented in this paper are obtained with fully absorbing boundary conditions, which in the absence of information about the experimental pressure profile in the downstream region is a reasonable choice for modeling a *pull* scenario, where the magnetic flux is pulled into the flux core. Preliminary exploration of partially reflecting boundary conditions shows that the thickness of the current layer is not affected appreciably by simple reflection of particles off the flux core surface.

The 2D simulations in this study are performed in the x-z plane and spatial gradients in y are not allowed in the evolution equations. The MRX poloidal field (PF) coils are modeled by prescribing, as a function of time, the out-of-plane current density in the two regions inside the flux cores, as shown in Fig. 1. The time dependence of the coil currents in the simulations is chosen to closely mimic the actual PF coils

$$I_{\mathrm{coil}}(t) = I_0[1 + 5\cos^2(\pi t/2\tau)]/6. \tag{2}$$

The characteristic time scale for the current ramp down τ represents the strength of the external drive, as discussed in Sec. III. The magnitude of the current I_0 is chosen to yield the desired value of electron beta $\beta_e=8\pi n_0 T_0/B_0^2$ at a reference position between the coils at $t=0$, where the reference value of the initial magnetic field created by the coils is B_0. The reference point is located at $(x,z)=(8.1,75)$ cm, as illustrated in Fig. 1. The initial distribution function for each species is a uniform Maxwellian $f_{s0}=n_0 m_s^{3/2}(2\pi T_0)^{-3/2}\exp[-m_s v^2/(2T_0)]$ with density n_0 and temperature T_0. This choice of the initial configuration represents the simplest possible assumption in the absence of detailed information on such parameters as initial global density profiles. Other choices of the initial configuration are possible and have been explored. In general, the initial configuration does not have to represent an exact equilibrium at $t=0$ since the relatively low-β plasmas adjust quickly to the given structure of the magnetic field and a dynamical quasi-equilibrium is typically established on a time scale of a few ion cyclotron times, which is much shorter than τ.

The computational requirements of the fully kinetic algorithm require the parameters of the real experiment to be scaled in order to obtain simulations of manageable size. We utilize the same scaling approach as in Ref. 6, namely, we try to match a set of relevant dimensionless parameters between the simulations and the experiment. In particular, the initial values of β_e, $\tau\Omega_{ci}^0$, and Z_0/d_i^0 are chosen to be close to the ones typically observed in the experiment. Here Z_0 is the distance between the flux cores, $d_s^0=c/\omega_{ps}^0$, $\omega_{ps}^0=(4\pi n_0 e^2/m_s)^{1/2}$, and $\Omega_{cs}=eB_0/(m_s c)$. Representative plasma parameters in MRX are $n=(0.1-1)\times 10^{14}$ cm^{-3}, $B=(100-500)G$, and $T_e=(1-10)$ eV, which imply $Z_0/d_i=(5.5-17.5)$ and $\beta_e=(0.01-2)$. Since we are interested in the electron dynamics, the collisionality is set by prescribing[22] the initial value of ν_e^0/Ω_{ce}^0 in the range of 0.01–0.25 characteristic of the experiment. Here $\nu_e^0=4\sqrt{2\pi}n_0\Lambda e^4/(3\sqrt{m_e}T_0^{3/2})$ is the electron collision frequency[12] and Λ is the Coulomb logarithm.

This scaling approach ensures that the reference value of Lundquist number in the simulation $S=(Z_0/d_i^0)\Omega_{ce}^0/\nu_e^0$ corresponds to that in the experiment. The dimensionless parameters that are not expected to strongly affect the reconnection

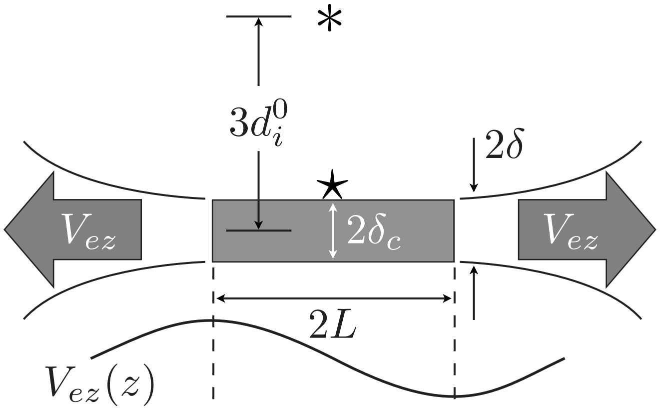

FIG. 2. A schematic of the electron reconnection layer illustrating the definition of various quantities used in the text. Here L refers to the length of the layer, as measured by the distance between the center of the layer and the z position corresponding to the maximum outflow speed V_{ez}; δ is the width of the outflow channel as measured by the width of V_{ez} profile at 40% of the maximum value at the z position corresponding to maximum outflow; δ_c refers to the width of the current profile at the center of the layer at 40% of the maximum value; $\star$ is the position at the inflow edge of the electron layer and $*$ is the position $3d_i^0$ upstream from the x-point.

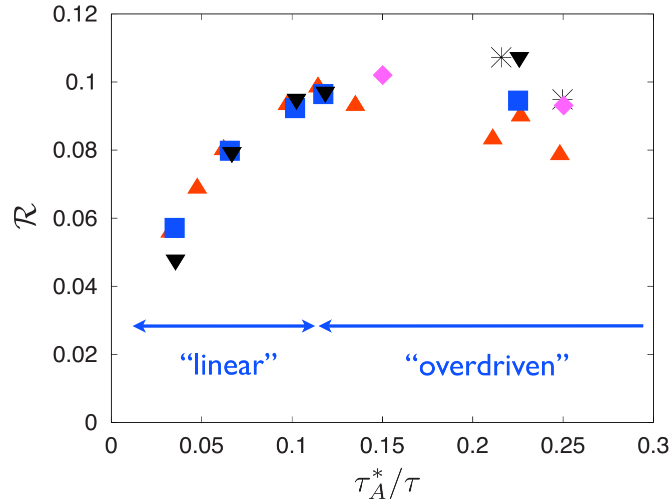

FIG. 3. (Color online) Reconnection rate [Eq. (3)] vs the strength of the drive τ_A^*/τ. The symbols denote the reference value of collisionality ν_e^0/Ω_{ce}^0 as follows 0 (▲), 0.012 (■), 0.06 (▼), 0.05 ($*$), and 0.25 (◆). The last two sets of simulations were performed at reference density $n_0=8\times10^{13}$ cm^{-3}, while the rest have $n_0=2\times10^{13}$ cm^{-3}. The mass ratio is $m_i/m_e=100$ for all the simulations shown.

physics are chosen to minimize the computational cost. For example, the value of $\omega_{pe}^0/\Omega_{ce}^0=2$ in contrast to typical MRX values $\omega_{pe}/\Omega_{ce}=70-80$. It is important to emphasize that the simulations do not attempt to reproduce the complicated dynamics of plasma formation and initial evolution in MRX (for example, the initial *push* phase is not modeled). Consequently, the values of some important parameters, such as β_e, plasma density, or the strength of the drive $\tau\Omega_{ci}$ defined with a local value of magnetic field during the time period where the reconnection layer is analyzed, may differ substantially from the initial reference values. Thus it is important to identify a set of dimensionless parameters that are critical *and* can be directly compared between simulations and the experiment (see Sec. IV).

The simulations are performed on a uniform Cartesian grid with a typical size of the computational cell equal to $(1-1.8)\lambda_D$, where λ_D is the Debye length based on the initial density and temperature. This corresponds to typical grid sizes $\Delta x\approx 0.2d_e^0$, translating to approximately 20 grid points across the thinnest current layer analyzed. The time step is limited by the Courant–Friedrichs–Lewy condition and a representative value is $\Delta t\omega_{pe}^0=0.15$. A typical initial number of particles per cell is 500. Finally, the ion-to-electron mass ratio is $m_i/m_e=100$ unless otherwise indicated. The dependence of the simulation results on the mass ratio is discussed in Sec. IV.

III. RECONNECTION RATE AND THE RECONNECTION MECHANISM

MRX is a driven system where the dynamics at macroscopic scales is forced by a clearly identifiable external driver in the form of PF coils. One of the basic questions in the study of reconnection is the coupling between the reconnection process, typically occurring at microscopic scales and the macroscopic dynamics. In the MRX configuration this issue can be examined by varying τ in Eq. (2), the time scale for the coil current ramp down. Since the experiment operates at relatively low values of β and the typical values of τ significantly exceed relevant MHD time scales, the inflow/outflow speed far enough from the reconnection site is to a large degree determined by the rate of change of the magnetic field generated by the PF coils. The plasma response may be quantified by considering the reconnection rate

$$\mathcal{R}=\left\langle\frac{cE_y}{B^*V_A^*}\right\rangle\approx\frac{\langle V_{\mathrm{in}}^*\rangle}{\langle V_A^*\rangle}. \tag{3}$$

Here $\langle\cdot\rangle$ refers to a time average (typically over a time interval $\Delta\mathcal{T}$ corresponding to $\Delta\mathcal{T}\Omega_{ci}^0\lesssim1$), E_y is the reconnection electric field at the x-point, V_{in} is the inflow plasma speed, $V_A=B/(4\pi nm_i)^{1/2}$, and quantities denoted by superscript * are measured at a location $3d_i^0$ upstream from the x-point (see Fig. 2 for a description of various definitions and characteristic locations used throughout the text). In the absence of plasma, the inductively generated electric field inside the simulation domain would scale as $E_y\propto Z_0B/(c\tau)$ and it is natural to introduce a dimensionless parameter describing the strength of the external drive as $\tau_A/\tau=Z_0/(\tau V_A)$. We will again use the superscript * to denote τ_A computed with the upstream values of density and magnetic field.

The dependence of the reconnection rate defined by Eq. (3) on τ_A^*/τ is shown in Fig. 3, which includes data from simulations with the reference collisionality varied in the range $\nu_e^0/\Omega_{ce}^0=0-0.25$, the drive time in the range $\tau\Omega_{ci}^0=35-300$, and the initial density of $n_0=(2-8)\times10^{13}$ cm^{-3}. The reconnection rate is measured at $t/\tau\approx0.5$, which corresponds to the peak drive, and is averaged over 100–500 time steps, corresponding to a time interval $\Delta\mathcal{T}\Omega_{ci}^0\lesssim1$. For all of the values of collisionality used in this study, the basic dependence of the rate on τ_A^*/τ remains similar, with two clearly identifiable regimes. In the *linear* regime the reconnection electric field scales linearly with the vacuum field E_v and the reconnection rate increases with τ_A^*/τ. In the *over-driven* or *saturated* regime the electric field at the center of the current sheet increases weakly with τ_A^*/τ, while the reconnection rate defined by Eq. (3) remains constant or even decreases with the increasing drive. Typical values of the rate in this regime are $\mathcal{R}\sim 0.1$. As is apparent from Fig. 3, the reconnection rate and the value of τ_A^*/τ corresponding to the transition between the linear and saturated regimes exhibit a rather weak dependence on the collisionality. The variations in the rate with ν_e/Ω_{ce} are somewhat larger in the saturated regime, where the rate varies by about 30% from collisionless simulations to those with $\nu_e/\Omega_{ce}\sim 0.1$. However, the apparent weak dependence of the reconnection rate on the collisionality should be taken with a considerable degree of caution. Indeed, the rather short spatial extent of the simulations in the outflow direction [approximately $(4-8)d_i$ depending on the density] constrains the maximum allowable length of the current sheet. Even the Sweet–Parker rate computed with a representative (high) value of the Lundquist number $S=500$ is $\mathcal{R}\approx 0.045$.

The simulations included in the present analysis span a wide range of collisionalities and it is instructive to analyze how the reconnection mechanism changes between collisionless simulations and those with the highest collisionality $\nu_e^0/\Omega_{ce}^0\sim 0.25$. To quantify this, we consider the y component of the electron momentum balance equation [v_y moment of Eq. (1)]

$$ne\left(\boldsymbol{E}+\frac{1}{c}\boldsymbol{V}_e\times\boldsymbol{B}\right)_y=-(\nabla\cdot\boldsymbol{P}_e)_y+R_y-m_e n\frac{dV_{ey}}{dt}, \qquad (4)$$

where

$$R_y\equiv m_e\int d^3v v_y \mathbb{C}\{f_e,f_i\} \qquad (5)$$

describes the collisional momentum exchange between electrons and ions and $\boldsymbol{P}_e$ is the electron pressure tensor. In short mean-free-path regimes (see, e.g., Ref. 12 for a more accurate discussion of the regions of validity) the transport theory relates $\boldsymbol{R}$ and $(\nabla\cdot\boldsymbol{P})$ to the low-order moments of the distribution function $(n,\boldsymbol{V},T)$, allowing a self-consistent closed set of fluid equations to be obtained. In general, such a closure cannot be achieved and a kinetic formalism that retains collision operator is required. Even in the regimes where the use of fluid equations is well justified, the general form of the momentum exchange R_y is considerably more complicated than simple relations typically used in fluid models of reconnection (see, e.g., Ref. 13 for a discussion in context of reconnection simulations).

In order to assess the relative role of various dissipation processes, all quantities in Eq. (4) with the exception of R_y were directly measured in the simulations at $t/\tau\approx 0.5$. To achieve good statistics, the measurements were averaged both in time over several hundreds of time steps and in space over a small box with dimensions of $(1-2)d_e^0$ located near the center of the current sheet. The collisional momentum exchange R_y was computed as the residual in Eq. (4) and similarly averaged. We have verified[13] that in the collisionless case the residual R_y is small [only a few percent of the dominant terms in Eq. (4)], while in the strongly collisional limit it is in excellent agreement with the theoretical predictions from collisional transport theory. It is well known that in sufficiently collisional regimes R_y is the dominant contribution on the right hand side of Eq. (4), while in the collisionless regimes the relevant effects are represented by $(\nabla\cdot\boldsymbol{P}_e)_y$. Thus it is not surprising that for all the values of collisionality considered the approximate force balance near the center of the current sheet is

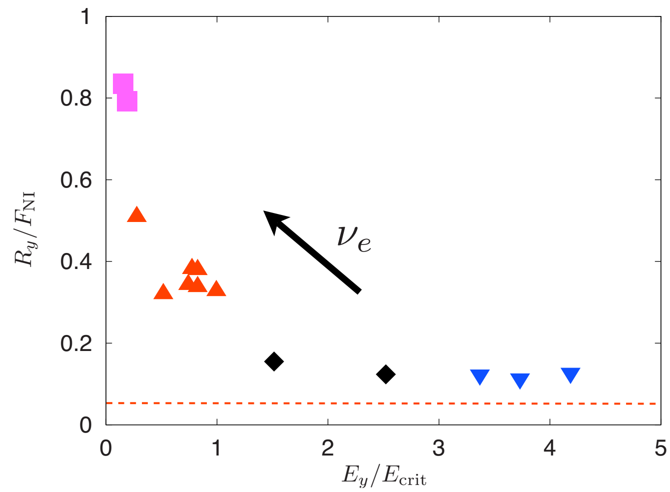

FIG. 4. (Color online) The portion of the nonideal electric field supported by the collisional momentum exchange between the electrons and ions vs the ratio between the reconnection electric field E_y and the runaway critical field $E_{\rm crit}$. The horizontal dashed line denotes approximate sensitivity of the diagnostic. The symbols denote the value of collisionality $\nu_e^c/\Omega_{ce}^\star$ as follows 0–0.025 (▼), 0.025–0.05 (◆), 0.05–0.1 (▲), and 0.1 and greater (■).

$$F_{\rm NI}\equiv n_e e\left(\boldsymbol{E}+\frac{1}{c}\boldsymbol{V}_e\times\boldsymbol{B}\right)_y\approx-(\nabla\cdot\boldsymbol{P}_e)_y+R_y. \qquad (6)$$

This is illustrated in Fig. 4, which shows the ratio $R_y/F_{\rm NI}$ as a function of $E_y/E_{\rm crit}$, the ratio between the reconnection electric field at the center of the box E_y and the runaway electric field

$$E_{\rm crit}\equiv\sqrt{T_e m_e}\nu_e/e. \qquad (7)$$

Figure 4 may be considered a diagram of the collisionality regimes. In weakly collisional regimes, corresponding to $E_y\gtrsim E_{\rm crit}$, the reconnection electric field is supported predominantly by the divergence of the electron stress tensor $(\nabla\cdot\boldsymbol{P}_e)_y$. As collisionality is increased, the momentum exchange between ions and electrons plays a more important role and up to 80% of the reconnection electric field is supported by R_y when $E_y\ll E_{\rm crit}$. A simple physical argument can be given that demonstrates how $E_y/E_{\rm crit}$ appears as a natural scale separating collisional reconnection regimes from collisionless ones. Indeed, in fully collisional regimes the electric field near the neutral line is supported by classical resistivity so $E_y\sim\eta j_y\sim(m_e\nu_e/ne^2)(cB/4\pi\delta)$. In collisionless regime, the electric filed is supported by $(\nabla\cdot\boldsymbol{P}_e)_y$, which can be estimated as $(\nabla\cdot\boldsymbol{P}_e)_y\sim ne(\sqrt{2m_eT_e}/e)V_{\rm out}/L$, where $V_{\rm out}$ is the outflow speed at the edge of the electron layer and L is the length of the layer.[6,26] Then from mass conservation

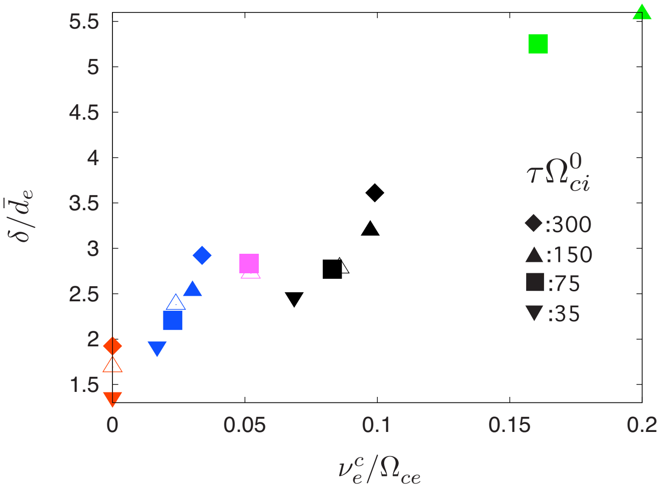

FIG. 5. (Color online) The dependence of the width of the layer $\delta/\bar{d}_e$ on collisionality $\nu_e^c/\Omega_{ce}^\star$. Here $\bar{d}_e$ is the collisionless electron skin depth defined with electron density line averaged over a distance corresponding to the flux core diameter. Collision frequency ν_e^c is defined with central temperature and density and $\Omega_{ce}^\star$ is defined with the value of magnetic field on the shoulder of the electron layer (see Fig. 2).

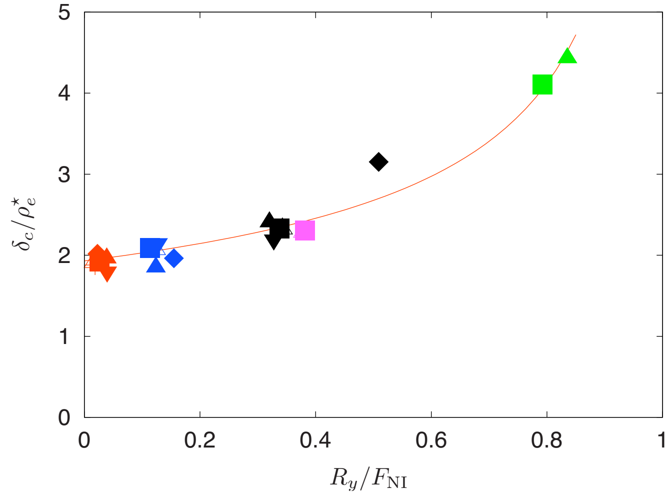

FIG. 6. (Color online) The dependence of the central width of the layer $\delta_c/\rho_e^\star$ on the dissipation mechanism, quantified by R_y/F_{NI}, the portion of the nonideal electric field supported by the collisional momentum exchange between the electrons and ions. Here δ_c refers to the width of the current profile j_y at the center of the layer and $\rho_e^\star$ is the electron gyroradius defined with the central temperature and the magnetic field at the shoulder of the electron layer (see Fig. 2). The meaning of the symbols is the same as in Fig. 5. The continuous line shows a fit of the data points to the function $f(x)=a(1-x)^{-b}$.

$V_{\mathrm{out}}\delta/L\approx(cE_y/B^\star)$ and one obtains that $\eta j_y\sim(\nabla\cdot\boldsymbol{P}_e)_y/(ne)$ when $E/E_{\mathrm{crit}}\sim 1/\beta_e^\star$. Here $\beta_e^\star=8\pi n_c T_e^c/(B^\star)^2$, the quantities denoted by $\star$ are measured at the inflow edge of the electron layer (see Fig. 2), and those denoted by c are measured at the center of the layer. Force balance across a typical layer ensures that $\beta_e^\star\sim 1$ so that a crossover between collisional and collisionless regimes may be expected when $E_y\sim E_{\mathrm{crit}}$. In reality, significant modifications in the electron distribution function and the associated breakdown of transport theory can be expected even when the electric field is substantially below E_{crit} so that the use of fluid models is rigorously justified only when $E_y\ll E_{\mathrm{crit}}$. It is also worth pointing out that the presence of Coulomb collisions modifies the $\nabla\cdot\boldsymbol{P}_e$ term, which contains contributions from viscosity in fully collisional regimes. However, there is no reliable method to separate the "collisional" and "collisionless" contributions to $\nabla\cdot\boldsymbol{P}_e$ in the simulation.

IV. THE STRUCTURE OF THE ELECTRON RECONNECTION LAYER

One of the major goals of the analysis presented in this paper is to understand whether 2D kinetic simulations with Coulomb collisions can reproduce the layer structure observed in MRX. As described in details in Sec. II, a fully kinetic treatment of the problem requires a range of compromises in terms of the parameters that are feasible (mass ratio, ω_{pe}/Ω_{ce}, etc.). Furthermore, the manner in which the plasma is formed in the actual experiment is quite complex and is not modeled in our study. This imposes additional uncertainties, for example, in the drive time, initial profiles of temperature and density, etc. Thus in order to make meaningful comparisons between simulations and the experiment, it is important to identify the minimal set of *critical* dimensionless parameters that affect the layer structure and can be directly compared between simulations and experiments.

Traditionally, the width of the electron layer in MRX has been characterized through the width of the electron outflow channel.[3–6] Specifically, the width of the electron layer δ is defined as the half width of the V_{ez} profile (at 40% of maximum) at the z position that corresponds to the maximum electron outflow speed, as illustrated in Fig. 2. The dependence of δ on collisionality and the drive time in simulations with mass ratio $m_i/m_e=100$ is summarized in Fig. 5. Compared to the collisionless case, the layers are approximately 50% broader for $\nu_e^c/\Omega_{ce}^\star\sim 0.02$ and approximately 75% broader for $\nu_e^c/\Omega_{ce}^\star\sim 0.05$. Here, the value of ν_e^c is computed using the parameters at the center of the electron layer, while $\Omega_{ce}^\star$ is defined with the magnetic field at the edge of the electron layer. As is apparent from Fig. 5, the quantity δ/d_e does not have a simple relation with collisionality and instead depends on several parameters, including the drive time, the value of electron beta, and the mass ratio.

A much simpler relation between the reconnection mechanism and the width of the layer can be established by considering the width of the current layer at its center, denoted by δ_c in Fig. 2, and choosing an appropriately defined electron gyroradius as the relevant scale length. Indeed, in collisionless regimes the layer thickness is determined by the electron crossing orbit scale. For a thin sheet, in which the current density is dominantly carried by electrons, the crossing orbit scale is of order $\rho_e^\star$, where $\rho_e^\star=(2T_e^c/m_e)^{1/2}/\Omega_{ce}^\star$, quantities measured at the center of the layer are again denoted by c, while those measured at the edge of the electron layer are denoted by superscript $\star$ (see Fig. 2). As demonstrated in Fig. 6, $\rho_e^\star$ remains the relevant scale length for the thickness of the layer in weakly collisional regimes, until a substantial portion of the reconnection electric field is supported by the collisional momentum exchange. Note that the electron gyroradius and the electron skin depth d_e are related by $\rho_e^\star/d_e=\beta_e^{1/2}$. Force balance across the electron layer requires $\beta_e=1-\beta_i+(\beta_e^\star+\beta_i^\star)$, where $\beta_s=8\pi n_c T_s^c/(B^\star)^2$ and $\beta_s^\star=8\pi n_\star T_s^\star/(B^\star)^2$. Typically, $\beta_e\lesssim 1$ in MRX, but many of the simulations in this study developed electron layers with $\beta_e^\star\gtrsim 1$ (especially at higher mass ratio) leading to $\beta_e>1$. If the width of the layer is measured in d_e, this introduces a misleading *thermal broadening* of the electron layer in the simulations, which would not occur in the experiment. One can account for this issue by simply using $\rho_e^\star$ to make comparisons.

As shown in Fig. 4, the ratio of the reconnection electric field to the runaway limit provides a convenient indication of the collisionality regime in the sense that it determines which nonideal terms dominate in Ohm's law. Thus in order to assess the role of Coulomb collisions in determining the layer structure observed in MRX, we can compare the latter between simulations and experiments with the same value of E_y/E_{crit}. An important implication of the scaling approach utilized in this study is that for a given collisionality ν_e/Ω_{ce} and a given reconnection rate $\mathcal{R}$ the ratio E_y/E_{crit} differs between simulations and the experiments. Indeed, this ratio can be estimated as $E_y/E_{\mathrm{crit}}\sim(\beta_e^*)^{-1/2}(m_e/m_i)^{1/2}(\Omega_{ce}^*/\nu_e^c)\mathcal{R}$, where Ω_{ce}^* and β_e^* are calculated with the magnetic field measured outside of the ion layer, while ν_e^c is calculated with the central density and electron temperature. Since the simulations employ a reduced mass ratio in the range $m_i/m_e=25-200$, the ratio E_y/E_{crit} is larger in our simulations compared to the experiment. If m_i/m_e was increased by *brute force* up to the hydrogen mass ratio, the parameter E_y/E_{crit} would be reduced and effectively matched to the experiment. However, this is not really necessary since the simulations were performed over a wide range of collisionalities and drive times thus covering an appropriate span of E_y/E_{crit}. The ratio E_y/E_{crit} has a clear physical interpretation, beautifully organizes our data over a wide range of parameters, and can be directly estimated in the experiments.

The dependence of $\delta_c/\rho_e^\star$ on the value of E_y/E_{crit} is shown in Fig. 7 for simulations with widely varying parameters, $m_i/m_e=25-200$, initial density corresponding to $n_0=(2-8)\times 10^{13}\ \mathrm{cm}^{-3}$, $\tau\Omega_{ci}^0=75-300$, and $\nu_e^0/\Omega_{ce}^0=0.01-0.1$. Two simple physical limits are also shown in Fig. 7. In the collisionless regime, the width of the current layer is given by the electron crossing orbit scale and is essentially constant in terms of $\rho_e^\star$. In the limit where the reconnection electric field is supported by classical resistivity, applicable when $E_y\ll E_{\mathrm{crit}}$, the width can be estimated as $\delta_c/\rho_e^\star\sim(\beta_e^\star)^{-1}(E_{\mathrm{crit}}/E_y)$. This limit may be relevant to more collisional MRX discharges with $E/E_{\mathrm{crit}}\lesssim 0.1$. The shaded region in Fig. 7 is bound by curves $\delta_c/\rho_e^\star=(\beta_e^\star)^{-1}(E_{\mathrm{crit}}/E_y)$ with $\beta_e^\star=0.5$, which is appropriate for MRX discharges, and $\beta_e^\star=1.5$, which is more appropriate for some of the simulations.

An important result summarized by Fig. 7 is that the width of the layer δ_c measured in terms of an appropriately defined electron gyroradius deviates from its collisionless value only when $E_y\ll E_{\mathrm{crit}}$. This is consistent with the physical understanding of reconnection with the electric fields approaching the runaway limit. Indeed, when the reconnection electric field approaches E_{crit}, the collisional momentum exchange becomes increasingly inefficient and a substantial portion of the nonideal electric field inside the electron layer must be supported by the off-diagonal terms in the electron stress tensor. On the other hand, electrons become magnetized on the length scale of the order of their meandering orbit width, which is of the order of $(\delta_c\rho_e^\star)^{1/2}$ if the thickness of the layer is δ_c. This implies that the off-diagonal terms in $\boldsymbol{P}_e$, representing the nongyrotropy of the distribution function, are diminished for layers that are substantially thicker than $\rho_e^\star$.

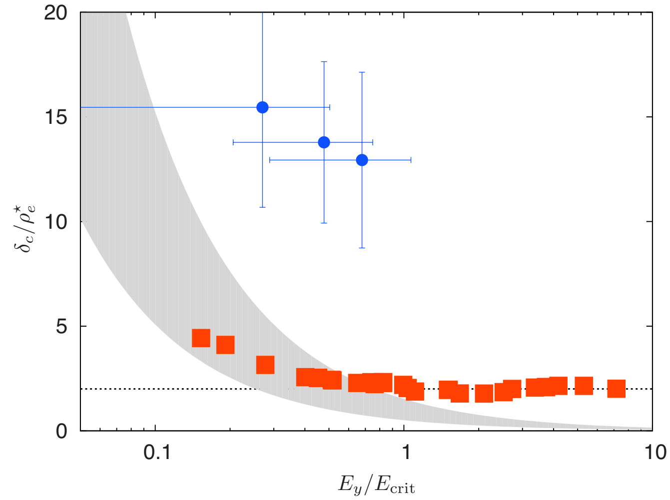

FIG. 7. (Color online) The dependence of the width of the layer normalized to electron gyroradius $\delta_c/\rho_e^\star$ on the ratio E_y/E_{crit}. Squares represent simulation results for a wide range of parameters, while MRX measurements are shown by filled circles. Two simple analytical limits for the dependence of $\delta_c/\rho_e^\star$ on E/E_{crit} are demonstrated. In the collisionless case $\delta_c/\rho_e^\star\approx$const, while in the limit where the reconnection electric field is supported by classical resistivity $\delta_c/\rho_e^\star\sim(\beta_e^\star)^{-1}(E_{\mathrm{crit}}/E_y)$. The latter limit is represented by the shaded region, which is bound by curves with $\beta_e^\star=0.5$ appropriate for MRX experiments and $\beta_e^\star=1.5$ appropriate for some of the simulations.

The prediction relating $\delta_c/\rho_e^\star$ and E_y/E_{crit} can be applied to the low-density discharges in MRX, where the reconnection electric field is comparable to E_{crit}. The filled circles in Fig. 7 represent the experimental measurements of the layer width in MRX discharges. In this case, the width was defined by fitting the $B_z(x)$ profile at a z location 3 cm away from the center to a function of the form $B_f(x)=B_c+B_L(x/\delta_c)+B_0\tanh(x/\delta_c)$, where B_c, B_L, and B_0 are constants. The layer length in MRX typically exceeds 3 cm and this measurement is close to the layer width at the center. The shown width of the layer in MRX regimes with $E\lesssim E_{\mathrm{crit}}$ is consistent with preliminary measurements of the layer width performed at the center of the layer (not shown). Each experimental data point in Fig. 7 represents the result of averaging over many similar discharges with error bars reflecting the statistical deviation of this averaging procedure. In addition to the shot-to-shot statistical variation, the results are potentially subject to a systematic error due to the current blockage by the probes,[3–5] which is expected to lead to an overestimation of the width by 5%–45%. Even with the maximal estimate of the systematic error, the experimental data points are substantially above the ones obtained from simulations. This indicates that in the presence of Coulomb collisions the width of the electron layers in 2D simulations is substantially below the experimentally measured values, which in turn implies that collisional effects in the 2D kinetic simulations cannot account for the electron layer thickness observed in MRX.

V. SUMMARY AND DISCUSSION

In this paper we have presented results concerning the influence of Coulomb collisions on the dynamics of driven magnetic reconnection and the structure of reconnection layers for the parameters and geometry mimicking the MRX. The analysis is motivated by the need to assess the role of collisions in the regimes where the collisional transport theory breaks down, but where collisions are sufficiently strong to play a significant role. The influence of Coulomb collisions on the structure of reconnection layers in MRX is of particular interest since previous 2D collisionless simulations[6] revealed a systematic discrepancy between the simulation results and the experimental observations concerning the width of the electron-scale layers, which were found to be several times thinner in the simulations. In order to address this discrepancy, 2D fully kinetic simulations with a Monte Carlo treatment of the collision operator were employed in the present study. This powerful simulation technique allows regimes with arbitrary collisionality to be analyzed. At the same time, the simulations necessarily make a number of compromises, for example, utilizing a simplified geometry, neglecting the processes of initial plasma formation, and employing reduced values of some potentially important parameters (m_i/m_e, ω_{pe}/Ω_{ce}, etc.). Thus comparison with experiments requires careful identification of the *minimal* set of important physical processes and understanding of how these processes can be modeled in simulation.

The simulations were performed for a range of collisionalities appropriate to conditions in MRX, and for a range of drive times τ controlling the characteristic time scale for ramp down of the MRX PF coils. Varying the latter allows a systematic examination to be performed of the relation between the strength of the drive and the reconnection rate. This relation represents a quantitative measure of the interplay between global large-scale dynamics and local reconnection physics. For all of the values of collisionality considered the rate exhibits the same qualitative behavior as a function of τ, previously reported in the collisionless limit.[6] In the linear regime, the reconnection electric field scales linearly with the driving electric field and the reconnection rate increases with $1/\tau$. In this regime, the value of the reconnection rate depends rather weakly on collisionality. In the saturated regime, the reconnection rate and the reconnection electric field show a much weaker dependence on the drive time. The variations in the rate with collisionality are larger than in the linear regime, but do not exceed 30%. The weak dependence of the rate on collisionality may be partially explained by a rather short spatial extent of the simulations in the outflow direction since the distance between the flux core surfaces is 40 cm, which corresponds to approximately $8d_i$ for $n=2\times10^{13}$ cm^{-3}. The relatively small size of the outflow region constraints the possibility of the layer expansion, which is known to be correlated with the reconnection rate (e.g., Refs. 27 and 28).

The changes in the reconnection mechanism in the presence of collisions were quantified by considering the out-of-plane component of the electron momentum balance equation (generalized Ohm's law). It is shown that in all the regimes analyzed the dominant terms balancing nonideal electric field at the center of the current layer are the divergence of the electron stress tensor $(\nabla\cdot\boldsymbol{P}_e)_y$ and the collisional momentum exchange between electrons and ions R_y. The ratio $(\nabla\cdot\boldsymbol{P}_e)_y/R_y$ is shown to depend crucially on the ratio between the reconnection electric field E_y and the runaway field E_{crit}, with R_y dominating in fluid regimes $E\ll E_{\text{crit}}$ and $\nabla\cdot\boldsymbol{P}_e$ dominating in weakly collisional regimes $E>E_{\text{crit}}$. The changes in the reconnection mechanism are related to the changes in the width of the current layer, which becomes wider when substantial portion of the reconnection electric field inside the current layer is supported by the collisional momentum exchange. However, a comparison of the simulation results with experimental observations indicates that Coulomb collisions alone are not sufficient to explain the observed width of the layer. Simulations predict that in the discharges with reconnection electric field of the order of the runaway limit the width of the layer should not substantially deviate from its collisionless value, which is of the order of an appropriately defined electron gyroradius $\rho_e^\star$. When applied to the experimental observations, this estimate is substantially below the measured values even with a maximal estimate of the systematic experimental error. For example, for $E_y=(0.4-1)E_{\text{crit}}$ the thickness of the layer found in simulations is $\delta_c=(2-3)\rho_e^\star$, while the thickness measured in the experiments is in the range $\delta_c\approx(10-15)\rho_e^\star$ with a systematic error due to the current blockage by the probes estimated to be 5%–45%.[3–5] This value of δ_c/ρ_e can be explained by 2D collisional simulations only if the electron temperature is two to three times lower than the measured value.

We thus conclude that 2D collisional simulations cannot account for the layer thickness observed in low-density MRX discharges. This makes it likely that physical processes beyond Coulomb collisions play a role in controlling the structure of reconnection layers in MRX. An interesting candidate for such a process is the presence of electromagnetic fluctuations that are routinely observed[29–31] in low-density MRX discharges with relatively large reconnection rates and have been identified in preliminary three-dimensional MRX simulations.[32]

ACKNOWLEDGMENTS

We gratefully acknowledge the support of the U.S. Department of Energy through the LANL/LDRD Program for this work. Contributions of H.K. were supported by the NASA Heliophysics Theory Program and NSF GEM Grant No. ATM 0802380 at UCSD. Simulations were performed with LANL institutional computing resources.

[1] M. Yamada, H. Ji, S. Hsu, T. Carter, R. Kulsrud, N. Bretz, F. Jobes, Y. Ono, and F. Perkins, Phys. Plasmas **4**, 1936 (1997); 38th Annual Meeting of the Division-of-Plasma-Physics of the American-Physical-Society, Denver, CO, 11–15 November 1996.

[2]Y. Ren, M. Yamada, S. Gerhardt, H. Ji, R. Kulsrud, and A. Kuritsyn, Phys. Rev. Lett. **95**, 055003 (2005).
[3]Y. Ren, M. Yamada, H. Ji, S. Gerhardt, and R. Kulsrud, Phys. Rev. Lett. **101**, 085003 (2008).
[4]Y. Ren, M. Yamada, H. Ji, S. Dorfman, S. P. Gerhardt, and R. Kulsrud, Phys. Plasmas **15**, 082113 (2008).
[5]H. Ji, Y. Ren, M. Yamada, S. Dorfman, W. Daughton, and S. P. Gerhardt, Geophys. Res. Lett. **35**, L13106, doi:10.1029/2008GL034538 (2008).
[6]S. Dorfman, W. Daughton, V. Roytershteyn, H. Ji, Y. Ren, and M. Yamada, Phys. Plasmas **15**, 102107 (2008).
[7]F. Trintchouk, M. Yamada, H. Ji, R. M. Kulsrud, and T. A. Carter, Phys. Plasmas **10**, 319 (2003).
[8]M. Yamada, Y. Ren, H. Ji, J. Breslau, S. Gerhardt, R. Kulsrud, and A. Kuritsyn, Phys. Plasmas **13**, 052119 (2006).
[9]A. Kuritsyn, M. Yamada, S. Gerhardt, H. Ji, R. Kulsrud, and Y. Ren, Phys. Plasmas **13**, 055703 (2006).
[10]A. Kuritsyn, H. Ji, S. P. Gerhardt, Y. Ren, and M. Yamada, Geophys. Res. Lett. **34**, L16106, doi:10.1029/2007GL030796 (2007).
[11]H. Ji, M. Yamada, S. Hsu, and R. Kulsrud, Phys. Rev. Lett. **80**, 3256 (1998).
[12]S. Braginskii, *Reviews of Plasma Physics* (Consultants Bureau, New York, 1965), Vol. 1, pp. 205–311.
[13]W. Daughton, V. Roytershteyn, B. J. Albright, H. Karimabadi, L. Yin, and K. J. Bowers, Phys. Plasmas **16**, 072117 (2009).
[14]Z. W. Ma and A. Bhattacharjee, Geophys. Res. Lett. **23**, 1673, doi:10.1029/96GL01600 (1996).
[15]J. Birn, J. F. Drake, M. A. Shay, B. N. Rogers, R. E. Denton, M. Hesse, M. Kuznetsova, Z. W. Ma, A. Bhattacharjee, A. Otto, and P. L. Pritchett, J. Geophys. Res., [Space Phys.] **106**, 3715, doi:10.1029/1999JA900449 (2001).
[16]P. A. Cassak, J. F. Drake, and M. A. Shay, Astrophys. J. **644**, L145 (2006).
[17]A. N. Simakov and L. Chacon, Phys. Rev. Lett. **101**, 105003 (2008).
[18]H. Dreicer, Phys. Rev. **115**, 238 (1959).
[19]H. T. Ji, T. Carter, S. Hsu, and M. Yamada, Earth, Planets Space **53**, 539 (2001).
[20]K. J. Bowers, B. J. Albright, B. Bergen, L. Yin, K. J. Barker, and D. J. Kerbyson, *Proceedings of the ACM/IEEE Conference on Supercomputing*, Austin, 2008 (IEEE, New York, 2008), pp. 1–11.
[21]K. J. Bowers, B. J. Albright, L. Yin, B. Bergen, and T. J. T. Kwan, Phys. Plasmas **15**, 055703 (2008).
[22]T. Takizuka and H. Abe, J. Comput. Phys. **25**, 205 (1977).
[23]D. S. Lemons, D. Winske, W. Daughton, and B. Albright, J. Comput. Phys. **228**, 1391 (2009).
[24]W. Daughton, V. Roytershteyn, B. J. Albright, H. Karimabadi, L. Yin, and K. J. Bowers, Phys. Rev. Lett. **103**, 065004 (2009).
[25]H. T. Ji, M. Yamada, S. Hsu, R. Kulsrud, T. Carter, and S. Zaharia, Phys. Plasmas **6**, 1743 (1999).
[26]M. Hesse, K. Schindler, J. Birn, and M. Kuznetsova, Phys. Plasmas **6**, 1781 (1999).
[27]W. Daughton, J. Scudder, and H. Karimabadi, Phys. Plasmas **13**, 072101 (2006).
[28]H. Karimabadi, W. Daughton, and J. Scudder, Geophys. Res. Lett. **34**, L13104, doi:10.1029/2007GL030306 (2007).
[29]H. T. Ji, S. Terry, M. Yamada, R. Kulsrud, A. Kuritsyn, and Y. Ren, Phys. Rev. Lett. **92**, 115001 (2004).
[30]T. A. Carter, H. Ji, F. Trintchouk, M. Yamada, and R. M. Kulsrud, Phys. Rev. Lett. **88**, 015001 (2002).
[31]T. A. Carter, M. Yamada, H. Ji, R. M. Kulsrud, and F. Trintchouk, Phys. Plasmas **9**, 3272 (2002).
[32]V. Roytershteyn, Bull. Am. Phys. Soc. **54**, 290 (2009), Paper TP8.00122.